Published in final edited form as:
Exp Oncol. 2009 June ; 31(2): 106–114.

IMAGE FUSION USING CT, MRI AND PET FOR TREATMENT PLANNING, NAVIGATION AND FOLLOW UP IN PERCUTANEOUS RFA

F.L. Giesel[1,2,3], **A. Mehndiratta**[2,4], **J. Locklin**[1], **M.J. McAuliffe**[5], **S. White**[6], **P.L. Choyke**[7], **M.V. Knopp**[8], **B.J. Wood**[1,9], **U. Haberkorn**[3], and **H. von Tengg-Kobligk**[1,2,8]

[1] Department of Radiology, Clinical Center, National Institutes of Health, Bethesda 20892, MD, USA

[2] German Cancer Research Center (dkfz), Department of Radiology, Heidelberg 69120, Germany

[3] Department of Nuclear Medicine, University of Heidelberg, Heidelberg 69117, Germany

[4] School of Medical Science and Technology, Indian Institute of Technology, Kharagpur 721302, India

[5] National Institutes of Health, Center for Information Technology, Bethesda 20892, MD, USA

[6] New Jersey School of Medicine, Newark, 07103 NJ, USA

[7] National Institutes of Health, Molecular Imaging Program, National Cancer Institute, Bethesda 20892, MD, USA

[8] The Ohio State University, Department of Radiology, Columbus 43210, OH, USA

[9] National Institutes of Health, Surgery Branch, National Cancer Institute, Bethesda 20892, MD, USA

Abstract

Aim—To evaluate the feasibility of fusion of morphologic and functional imaging modalities to facilitate treatment planning, probe placement, probe re-positioning, and early detection of residual disease following radiofrequency ablation (RFA) of cancer.

Methods—Multi-modality datasets were separately acquired that included functional (FDG-PET and DCE-MRI) and standard morphologic studies (CT and MRI). Different combinations of imaging modalities were registered and fused prior to, during, and following percutaneous image-guided tumor ablation with radiofrequency. Different algorithms and visualization tools were evaluated for both intra-modality and inter-modality image registration using the software MIPAV (Medical Image Processing, Analysis and Visualization). Semi-automated and automated registration algorithms were used on a standard PC workstation: 1) landmark-based least-squares rigid registration, 2) landmark-based thin-plate spline elastic registration, and 3) automatic voxel-similarity, affine registration.

Results—Intra- and inter-modality image fusion were successfully performed prior to, during and after RFA procedures. Fusion of morphologic and functional images provided a useful view of the spatial relationship of lesion structure and functional significance. Fused axial images and segmented three-dimensional surface models were used for treatment planning and post-RFA evaluation, to assess potential for optimizing needle placement during procedures.

*Correspondence: Fax: +49-6221-422462, f.giesel@dkfz.de.

Conclusion—Fusion of morphologic and functional images is feasible before, during and after radiofrequency ablation of tumors in abdominal organs. For routine use, the semi-automated registration algorithms may be most practical. Image fusion may facilitate interventional procedures like RFA and should be further evaluated.

Keywords

image fusion; radiofrequency ablation; registration; registration algorithms; treatment planning

The value of image processing and fusion has been investigated for diagnostic and prognostic purposes; still it has been a less studied tool for interventional radiological procedures. Registration and fusion of radiological images is by no means a new post processing technique [1–5]. There are numerous technical approaches described to coalesce imaging data from different modalities [6–8] and use them to provide better health care for the patient. Registration is defined as aligning the two imaging data sets spatially to each other. While fusion is defined as overlaying them and visualizing them as one image. Algorithms for registration of anatomical and functional data sets have been mostly studied in fixed or rigid organs such as the spine or brain [2,4,7,9,10]. But registration is somewhat more difficult in region with physiologic movements like the neck [11] or in moving organs such as lungs [12,13]. Major challenges due to physiologic motion and the non-rigid nature of organs have limited the practical implementation of image fusion for abdominal interventional procedures for diagnostic and prognostic reasons.

Recent studies have shown that fusion of abdominal images from different modalities can improve diagnosis and monitoring of disease progression [14–16]. New hybrid-imaging systems combining positron emission tomography (PET) or single photon emission computed tomography (SPECT) with computed tomography (CT) offer a one-stop examination promoting the diagnostic and prognostic potentials for extra-cranial applications of image fusion in cancer [17–21]. Image fusion has proven useful for evaluation of patients with cancer supporting diagnosis, staging, treatment planning, monitoring the response to therapy including disease progression [22]. Minimally invasive image-guided therapy like radiofrequency thermal ablation is being routinely used, especially in the liver, lung, bone and kidney [23–26] and improves survival for certain patients [27].

Optimal outcomes of percutaneous radiofrequency ablation (RFA) are highly dependent upon accurate targeting of the neoplastic tissue and monitoring of the resulting thermal lesion. Success of treatment is intimately linked to the volumetric spatial relationship of neoplastic tissue to the thermal lesion margins. An accurate spatial understanding of this relationship that is readily accessible may provide feedback during pre-treatment planning, procedural navigation, early detection of re-growth improving prognosis. Ideal image guidance for RFA allows accurate probe placement for sphere-packing with sufficient overlap to avoid gaps of sub-lethal heating, and to treat a small margin of normal tissue beyond the neoplastic tissue borders. This is a challenging task and is prone to human error. The procedure is to be followed by repeated scanning and look for disease progression.

Image fusion was studied with an image processing software used before, during, and after RFA interventions. Fusion of morphologic and functional image data might improve spatial appreciation and visualization of tumor and its relation to thermal lesion margins.

MATERIAL AND METHODS

All reported patients were enrolled under investigational protocols that were approved by the Investigational Review Boards (IRB) of the NIH. Written informed consent was obtained from

all patients prior to the procedures. For this report patients and images were selected if they could demonstrate the feasibility and value of the presented fusion technique.

Imaging modalities

Morphologic imaging was performed with and without contrast enhancement using CTi and Light Speed CT (GE Medical Systems, Milwaukee, WI) and 1.5 Tesla magnetic resonance imaging (MRI) (GE Medical Systems, Milwaukee, WI). Functional imaging included fluoro-18 labeled deoxyglucose (FDG)-PET (GE Medical Systems, Milwaukee, WI) and Dynamic Contrast enchanced (DCE)-MRI using the above mentioned scanner. Prior to RFA (pre-treatment phase) each patient underwent a contrast-enhanced CT. Some patients also had PET and contrast enhanced MRI or DCE-MRI scans. After the initial RFA treatment was completed, a 50–100 ml bolus of iodinated contrast medium was administered intravenously and a CT of the target organ was performed (procedural phase). After two month patients were followed up with CT and in some cases additionaly with PET or DCE-MRI (Post-treatment phase).

Data flow and image post processing—Source data was archived on the hospital picture archive and communication system (PACS, Kodak, Rochester, NY) in the standard imaging DICOM (Digital imaging and communications in medicine) format (Fig. 1). Relevant data sets were retrieved from the PACS onto a personal computer (PC) workstation (1.4 GHz processor, 512 MB RAM, MS Windows® 2000 Professional).

Image fusion of morphologic and functional data was performed prior, during and after RFA between the same (intra-modality) and different modalities (inter-modality) (Fig. 2). Intra- and inter-modality registration was carried out using both semi-automated landmark-based methods least squares [28], thin-plate-splines [29] and automatic voxel-similarity method, an optimized automated registration (OAR) [30,31], available in the application MIPAV (Medical Image Processing and Visualization, National Institutes of Health, Bethesda, MD) using the above described workstation. Registration algorithms used included: 1) least-squares rigid registration, 2) thin-plate spline elastic registration, and 3) automated voxel-similarity measure affine registration using either correlation ratio or mutual information cost functions. Intra-modality registration of pre- and post-treatment CT datasets was accomplished using an automatic affine (12 degrees of freedom) registration algorithm. This intra-modality image fusion process used a correlation-ratio voxel-simularity cost function to guide the registration of the images. To enhance the visualization of two fused images, MIPAV provides many tools that allow the user to independently personalize the contrast, brightness and lookup tables for each dataset. Adjustment and blending the amount each image contributes to the final combined display can be performed in real-time.

Different thresholds and color lookup-tables were evaluated for visualization regarding the imaging modality and combination of data sets. Image fusion, volume and surface rendering including multi-planar visualization were performed on the same workstation using the above mentioned MIPAV software.

A laptop PC (1.4 GHz processor, 512 MB RAM, Windows® 2000 Professional) was used for intra-procedural fusions and for intra-procedural display (see Fig. 1).

RESULTS

Fusion results varied in accuracy depending upon organ shift, respiratory variations, lesion or organ shrinkage, and positional changes. The semi-manual landmark methods (least squares, thin-plate splines) required longer setup times due to selection of landmarks (~10–20 min without cropping). This was less practical for intra-procedural navigation, and required a

trained user. However, applying the automated voxel-similarity affine registration algorithm to cropped volumes produced reasonable processing times, facilitating fusion during treatments (3–5 min with cropping). Cropping the image had two major advantages: first, cropping significantly reduced processing time and second, cropping localized the registration of the images, reducing non-linear distortion artifacts, thus improving the affine registration process. The voxel-similarity registration technique was the fastest and thus potentially most useful method for registration during treatments (Fig. 3). However, the landmark methods have a built-in internal control, and were better in selected cases for specific patients (Fig. 4, 5). The landmark-based elastic method (thin plate spline) was more accurate for registration of organ shift in some cases (Fig. 6). However, elastic methods alter the actual imaging data, and thus have potential for error.

Pre-treatment phase

The CT scans provided primarily morphologic information on organ anatomy, tumor environment, adjacent large vasculature, and vascular supply (see Fig. 3; 4, *a*). Functional imaging by PET and DCE-MRI scans allowed functional lesion assessment of the metabolic (see Fig. 4, *b*) or pharmacokinetic microvascular status of the lesion (see Fig. 5, *a*). RFA needle trajectories were planned based on conventional mental registration, and retrospectively validated with fused images (see Fig. 6, *b*; Fig. 7). In addition, fused 3D-images with PET or DCE-MRI confirmed or facilitated neoplastic targets. Volume rendering of lesions helped to understand the spatial relation of the tumor and surrounding structures, which was not obvious from the conventional two-dimensional view (see Fig. 4, *d*). Similar fused combinations localized suspicious residual tumor that would need repeated RFA (see Fig. 5, 6, *c*). DCE-MRI showed suspicious residual untreated tumor (see Fig. 5, *a*), which was confirmed with pre treatment PET fused to pre treatment CT (Fig. 5, *b*).

Procedural phase—Fused images especially helped to guide RFA in patients were CT alone could not define recurrent tumor (see Fig. 6, *c* and *d*) The procedural images were registered to the pre-treatment images. Fused images of pre-treatment-CT and intra-procedural post-RFA CT rapidly defined adequate treatment margins well using OAR technique (see Fig. 7).

If questionable areas are identified with possible residual tumor, then repeated RFA can be considered before the patient is removed from the room, although fusion was not used prospectively in our study to alter any treatment plan.

Post-treatment phase

Conventional assessment is based on a visual comparison to determine whether the pre-treatment lesions and post-treatment areas are well matched (see Fig. 3, *a* and *b*). However, registered and fused images may provide better visualization of subtle differences (see Fig. 3, *c* and *d*; 7, 8, 9). Follow-up imaging can be fused to pre-RFA imaging to compare tumor to treatment margin, however this method becomes less useful the longer the follow-up, given that post-RFA lesions will shrink with time (see Fig. 9).

Technical Results—Free network flow of DICOM images was achieved between PACS, imaging scanners and PC workstations. MIPAV provided both volume rendering as well as multi-planar display of fused images for lesion visualization with CT, MRI and PET datasets. Rigid (see Fig. 4; 9, *a–c*) and elastic (see Fig. 3, Fig. 9, *d–f*) registration methods were successfully applied intra-operatively but can be challenged due to organ shrinkage at follow up. Choosing accurate and homologous landmarks, in each of the volume datasets was rather time consuming, even more for inter modality registration e.g. PET-CT. The OAR method was faster and appreciated during the procedural phase. Cropping the image had two major advantages; first, cropping significantly reduced processing time. Second, cropping localized

the registration, reducing non-linear distortion artifacts, thus improving the affine registration process by narrowing the processing to the volume of interest.

DISCUSSION

Previous studies have shown that image fusion is a powerful methodology to enhance diagnostic and follow up imaging in cancer patients [30,32–34]. Different registration algorithms have been used successfully for non-interventional applications in the past [29, 35], and were successfully applied in this study to RFA for liver and kidney tumors. Registration and fusion may be useful during interventional procedures and may assist before, during, and after RFA [21]. Often morphologic and functional imaging studies provide separate and complimentary information. Registration of pre- and post-RFA images may provide another window into the often-subtle spatial relationships between tumor and post-RFA thermal lesion. Conventional interpretation uses mental registration [9]; however computer processing may provide a more objective and exact view [36]. Image fusion has matured predominately for rigid structures (brain and bone), and many technical details have already been refined, however, several major problems remain while performing image fusion after RFA.

The problem of respiratory motion is inherent to the imaging itself. Image fusion is easily performed on the brain [2] because the skull is a rigid structure that prohibits significant movements. Unlike the brain, the abdominal cavity is not stationary, and organs can significantly alter their shape and location. These changes can be due to breathing, the position of the patient on the table, organ shift, change in organ shape, hydration status, stomach contents, and the RFA procedure itself etc. Not surprisingly, this caused mis-registration and hampered the fusion process in the kidney and liver in some cases.

Organ shift and shrinkage were encountered, as thermal lesions tend to shrink after RFA. This is problematic for retrospective fusion of post-RFA images to pre-RFA images to assess for adequacy of treatment margin (see Fig. 9). If weeks to months are allowed to pass before post-RFA imaging, then registration may show the now-shrunken thermal lesion to be smaller than the tumor, giving the false impression of inadequate treatment. This occurred repeatedly when we compared 2-month post-RFA images to pre-RFA images in kidney tumor patients, who did not suffer subsequent recurrence years later (see Fig. 7).

The size of the safety margin may influence the utility of this technique [37]. In the liver, a 5–10 mm margin of normal tissue burned may be easier to mentally co-register than a patient with a familial renal cell carcinoma, where only a several mm margin is desirable, to preserve normal kidney function given the predisposition for synchronous and metachronous tumor development over a lifetime. For the latter, this technique may be more useful.

If a tumor only presents during arterial phase imaging, co-registration may enable using the spatial information of that brief arterial phase for localization during a procedure. Image registration lets the physician use off-line prior imaging in the procedure room. Any imaging dataset can be registered to CT space, which can then be used to guide robotic needle placements for point and click tumor destruction [38]. This is a powerful tool that may gain importance in the future as tumor-specific and cell-specific contrast agents are developed. Fusion may also enable biopsy of metabolically active regions of a tumor, which could facilitate more accurate biopsy and improved information on the temporal and spatial evolution of a tumor genomic or proteomic profile. This in turn could help tailor patient-specific drug regimens.

Region cropping proved to be a rapid and simple method of scaling down the large imaging datasets into a computationally workable size. While future optimizations are planned and

processing speeds are improving, the registration process took 3–5 min, which makes this technique clinically relevant for intra-procedural monitoring and navigation. Monitoring and navigation during RFA currently suffers from imaging limitations. Ultrasound gas shadows the burn, CT contrast increases risk of renal toxicity, CT fluoroscopy has potentially high radiation doses to the user, and MR thermometry is not widely available, is costly, and requires a RF switch box or alternating imaging Rf-signals with treatment currents. Electromagnetic tracking during RFA may register pre-procedural imaging to the patient for use during needle manipulation and is being further investigated as an alternate method allowing use of pre-procedural imaging during interventions [39].

Versatile fusion software with multiple available methods of rigid and elastic registration may improve chances for optimal fusion for a given patient [40,41], as each method has own inherent strengths and weaknesses. However, fusion can facilitate interventions in select scenarios. Further validation is indicated before these techniques can be routinely utilized or applied to navigation systems or treatment planning software.

Current methods of monitoring treatment during RFA are inadequate and may represent the largest technical limitation of RFA today. Early detection of the tumor activity could potentially improve outcomes by allowing for early repeat intervention before regrowth results in a geometrically-unfavorable configuration.

In addition, method 1 (least squares) generates a rigid transformation, which involves 6 degrees of freedom (3 rotations and 3 translations). Method 2 (thin plate splines) is non-linear and can provide a richer registration than method 1 since this method can address non-linear registration problems (e. g., breathing artifacts, organ shift, and organ deformation). However, the accuracy of these two landmark registration methods is sensitive to user training and expertise in choosing landmarks. In addition, it can be time consuming and difficult to find enough landmarks to produce and acceptable registration.

However, the affine voxel-similarity automatic method is invariant to the user and often provides an acceptable result. This method has up to 12 degrees of freedom (3 rotations, 3 translations, 3 scale and 3 skew). While this may yield useful results, this method does not address breathing artifacts very well. Voxel similarity methods use statistics based on comparisons of voxel intensities between two datasets. Correlation ratio and cross-correlation measures are typically used to register intra-modality datasets. Normalized mutual information is typically used for inter-modality registration. Correlation ratio and normalized mutual information cost functions were used in this study for method 3 for intra and inter modality registration, respectively.

To fully visualize two fused images, it is important to be able to adjust the colorization or lookup tables, brightness, and contrast of each image independently. In addition, it is also important to be able to adjust the amount of blending between the two fused images. Having the ability to modify these image attributes greatly improves the visualization of lesions, vessels, and necrotic tissue. Such visualization is vital to the accurate assessment of RFA safety margins (see Fig. 3 and Fig. 7). The most subjectively effective color schemes were saved, which allowed the further automation of routine post-processing steps. In addition, surface-rendering techniques allowed for localization and the visual quantification of both pre-treatment lesion and post-treatment ablation volumes. Image processing and multimodality fusion are mature diagnostic tools that should be further evaluated for potential utility during interventional radiology procedures.

Acknowledgments

This work was supported in part by the Intramural Research Program of the NIH.

The authors thank Stephen Bacharach, MD, Ingmar Bitter, PhD and Grace Ko, MD for their support.

Abbreviations used

CT	computed tomography
DCE	dynamic contrast enhanced
DICOM	digital imaging and communications in medicine
FDG-PET	[F-18] 2-deoxy-2-fluoro-D-glucose positron emission tomography
Gd-DTPA	gadolinium diethylene-triamine-penta-acetic acid
MRI	magnetic resonance imaging
PACS	picture archiving and communication system
RFA	radiofrequency ablation

References

1. Kramer EL, Noz ME, Sanger JJ, et al. CT-SPECT fusion to correlate radiolabeled monoclonal antibody uptake with abdominal CT findings. Radiology 1989;172:861–5. [PubMed: 2788895]
2. Pietrzyk U, Herholz K, Fink G, et al. An interactive technique for three-dimensional image registration: validation for PET, SPECT, MRI and CT brain studies. J Nucl Med 1994;35:2011–8. [PubMed: 7989986]
3. Wahl RL, Quint LE, Cieslak RD, et al. "Anatometabolic" tumor imaging: fusion of FDG PET with CT or MRI to localize foci of increased activity. J Nucl Med 1993;34:1190–7. [PubMed: 8315501]
4. Mountz JM, Zhang B, Liu HG, Inampudi C. A reference method for correlation of anatomic and functional brain images: validation and clinical application. Semin Nucl Med 1994;24:256–71. [PubMed: 7817199]
5. Correia JA. Registration of nuclear medicine images. J Nucl Med 1990;31:1227–9. [PubMed: 2362202]
6. Maintz JB, Viergever MA. A survey of medical image registration. Med Image Anal 1998;2:1–36. [PubMed: 10638851]
7. Viergever MA, Maintz JB, Stokking R. Integration of functional and anatomical brain images. Biophys Chem 1997;68:207–19. [PubMed: 9468620]
8. Cai J, Chu JC, Recine D, et al. CT and PET lung image registration and fusion in radiotherapy treatment planning using the chamfer-matching method. Int J Radiat Oncol Biol Phys 1999;43:883–91. [PubMed: 10098445]
9. Ferrari de Oliveira L, Azevedo Marques PM. Coregistration of brain single-positron emission computed tomography and magnetic resonance images using anatomical features. J Digit Imaging 2000;13:196–9. [PubMed: 10847399]
10. Sobottka SB, Bredow J, Beuthien-Baumann B, et al. Comparison of functional brain PET images and intraoperative brain-mapping data using image-guided surgery. Comput Aided Surg 2002;7:317–25. [PubMed: 12731094]
11. Schoder H, Yeung HW, Gonen M, et al. Head and neck cancer: clinical usefulness and accuracy of PET/CT image fusion. Radiology 2004;231:65–72. [PubMed: 14990824]
12. Katyal S, Kramer EL, Noz ME, et al. Fusion of immunoscintigraphy single photon emission computed tomography (SPECT) with CT of the chest in patients with non-small cell lung cancer. Cancer Res 1995;55:5759s–63s. [PubMed: 7493342]
13. D'Amico TA, Wong TZ, Harpole DH, et al. Impact of computed tomography-positron emission tomography fusion in staging patients with thoracic malignancies. Ann Thorac Surg 2002;74:160–3. [PubMed: 12118750]
14. Forster GJ, Laumann C, Nickel O, et al. SPET/CT image co-registration in the abdomen with a simple and cost-effective tool. Eur J Nucl Med Mol Imaging 2003;30:32–9. [PubMed: 12483407]

15. Goerres GW, Burger C, Schwitter MR, et al. PET/CT of the abdomen: optimizing the patient breathing pattern. Eur Radiol 2003;13:734–9. [PubMed: 12664111]
16. Antoch G, Kanja J, Bauer S, et al. Comparison of PET, CT, and dual-modality PET/CT imaging for monitoring of imatinib (STI571) therapy in patients with gastrointestinal stromal tumors. J Nucl Med 2004;45:357–65. [PubMed: 15001674]
17. Keidar Z, Israel O, Krausz Y. SPECT/CT in tumor imaging: technical aspects and clinical applications. Semin Nucl Med 2003;33:205–18. [PubMed: 12931322]
18. Israel O, Mor M, Gaitini D, et al. Combined functional and structural evaluation of cancer patients with a hybrid camera-based PET/CT system using (18)F-FDG. J Nucl Med 2002;43:1129–36. [PubMed: 12215549]
19. Seemann MD. PET/CT: fundamental principles. Eur J Med Res 2004;9:241–6. [PubMed: 15257877]
20. Townsend DW, Carney JP, Yap JT, Hall NC. PET/CT today and tomorrow. J Nucl Med 2004;45:4S–14S. [PubMed: 14736831]
21. Yap JT, Carney JP, Hall NC, Townsend DW. Image-guided cancer therapy using PET/CT. Cancer J 2004;10:221–33. [PubMed: 15383203]
22. Israel O, Keidar Z, Iosilevsky G, et al. The fusion of anatomic and physiologic imaging in the management of patients with cancer. Semin Nucl Med 2001;31:191–205. [PubMed: 11430526]
23. Wood BJ, Ramkaransingh JR, Fojo T, et al. Percutaneous tumor ablation with radiofrequency. Cancer 2002;94:443–51. [PubMed: 11900230]
24. Gervais DA, McGovern FJ, Arellano RS, et al. Renal cell carcinoma: clinical experience and technical success with radio-frequency ablation of 42 tumors. Radiology 2003;226:417–24. [PubMed: 12563135]
25. Thanos L, Mylona S, Pomoni M, et al. Primary lung cancer: treatment with radio-frequency thermal ablation. Eur Radiol 2004;14:897–901. [PubMed: 14666377]
26. Goetz MP, Callstrom MR, Charboneau JW, et al. Percutaneous image-guided radiofrequency ablation of painful metastases involving bone: a multicenter study. J Clin Oncol 2004;22:300–6. [PubMed: 14722039]
27. Jiao LR, Hansen PD, Havlik R, et al. Clinical short-term results of radiofrequency ablation in primary and secondary liver tumors. Am J Surg 1999;177:303–6. [PubMed: 10326848]
28. Arun KS, Huang TS, Blostein SD. Least-square fitting of two 3d point sets. IEEE Trans Pattern Anal Machine Intell 1987;9:698–700.
29. Rohr K, Stiehl HS, Sprengel R, et al. Landmark-based elastic registration using approximating thin-plate splines. IEEE Trans Med Imaging 2001;20:526–34. [PubMed: 11437112]
30. Faulhaber P, Nelson A, Mehta L, O'Donnell J. The Fusion of anatomic and physiologic tomographic images to enhance accurate interpretation. Clin Positron Imaging 2000;3:178. [PubMed: 11150781]
31. Jenkinson M, Smith S. A global optimization method for robust affine registration of brain images. Medical Image Analysis 2001;5:143–56. [PubMed: 11516708]
32. Mutic S, Palta JR, Butker EK, et al. Quality assurance for computed-tomography simulators and the computed-tomography-simulation process: report of the AAPM Radiation Therapy Committee Task Group No 66. Med Phys 2003;30:2762–92. [PubMed: 14596315]
33. Scott AM, Macapinlac H, Zhang JJ, et al. Clinical applications of fusion imaging in oncology. Nucl Med Biol 1994;21:775–84. [PubMed: 9241654]
34. Turkington TG, Jaszczak RJ, Pelizzari CA, et al. Accuracy of registration of PET, SPECT and MR images of a brain phantom. J Nucl Med 1993;34:1587–94. [PubMed: 8355080]
35. Meyer CR, Boes JL, Kim B, et al. Demonstration of accuracy and clinical versatility of mutual information for automatic multimodality image fusion using affine and thin-plate spline warped geometric deformations. Med Image Anal 1997;1:195–206. [PubMed: 9873906]
36. Vannier MW, Gayou DE. Automated registration of multimodality images. Radiology 1988;169:860–1. [PubMed: 3263667]
37. Berber E, Siperstein A. Local recurrence after laparoscopic radiofrequency ablation of liver tumors: an analysis of 1032 tumors. Ann Surg Oncol 2008;15:2757–64. [PubMed: 18618182]

38. Wood BJ, Banovac F, Friedman M, et al. CT-integrated programmable robot for image-guided procedures: comparison of free-hand and robot-assisted techniques. J Vasc Interven Radiol 2003;14:62.

39. Wood BJ, Zhang H, Durrani A, et al. Navigation with electromagnetic tracking for interventional radiology procedures: a feasibility study. J Vasc Interv Radiol 2005;16:445–7. [PubMed: 15802442]

40. Archip N, Tatli S, Morrison P, et al. Non-rigid registration of pre-procedural MR images with intra-procedural unenhanced CT images for improved targeting of tumors during liver radiofrequency ablations. Med Image Comput Comput Assist Interv Int Conf Med Image Comput Comput Assist Interv 2007;10:969–77.

41. Fujioka C, Horiguchi J, Ishifuro M, et al. A feasibility study: evaluation of radiofrequency ablation therapy to hepato-cellular carcinoma using image registration of preoperative and postoperative CT. Acad Radiol 2006;13:986–94. [PubMed: 16843851]

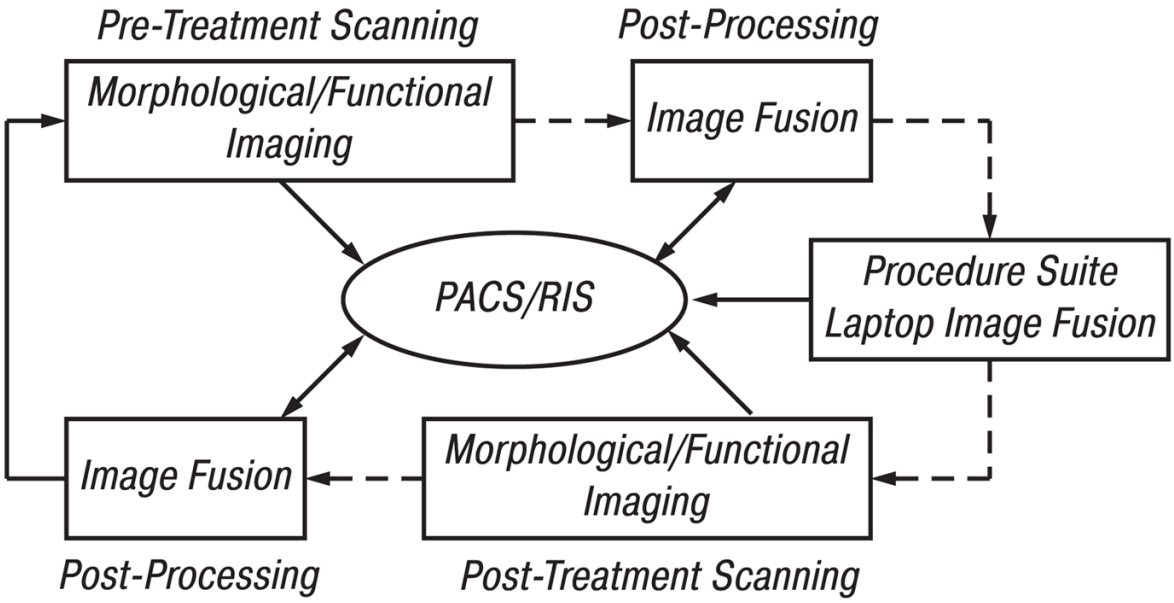

Fig. 1.

Workflow for patients scheduled for RFA. Initial imaging includes morphologic and/or functional imaging. DICOM images are sent directly or via PACS to a PC workstation for image registration and fusion. The results are pushed to a laptop that is taken into the procedure suite where patient information can be retrieved. During RFA, image fusion can be performed on the laptop, which may receive data from PACS or CT scanner. Follow-up morphologic and functional imaging data is later fused with pre-procedure imaging data on a workstation

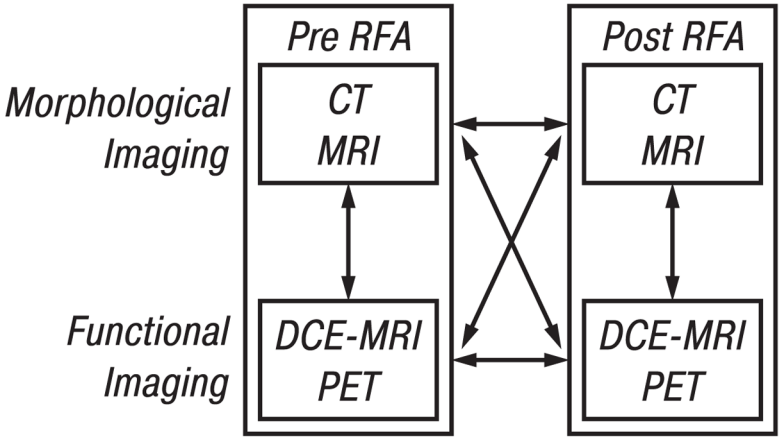

Fig. 2.

Image fusion combines the visualization characteristics of malignant lesions seen with morphologic (CT, MRI) and functional (PET, DCE-MRI) imaging before, during, and after RFA. After RFA the relation and characteristics of tumor and thermal lesion can be assessed in a fused data set. Various combinations are possible, including intra-modality (e. g. pre-CT *vs* post-CT) or inter-modality (e. g. pre-CT *vs* pre-PET)

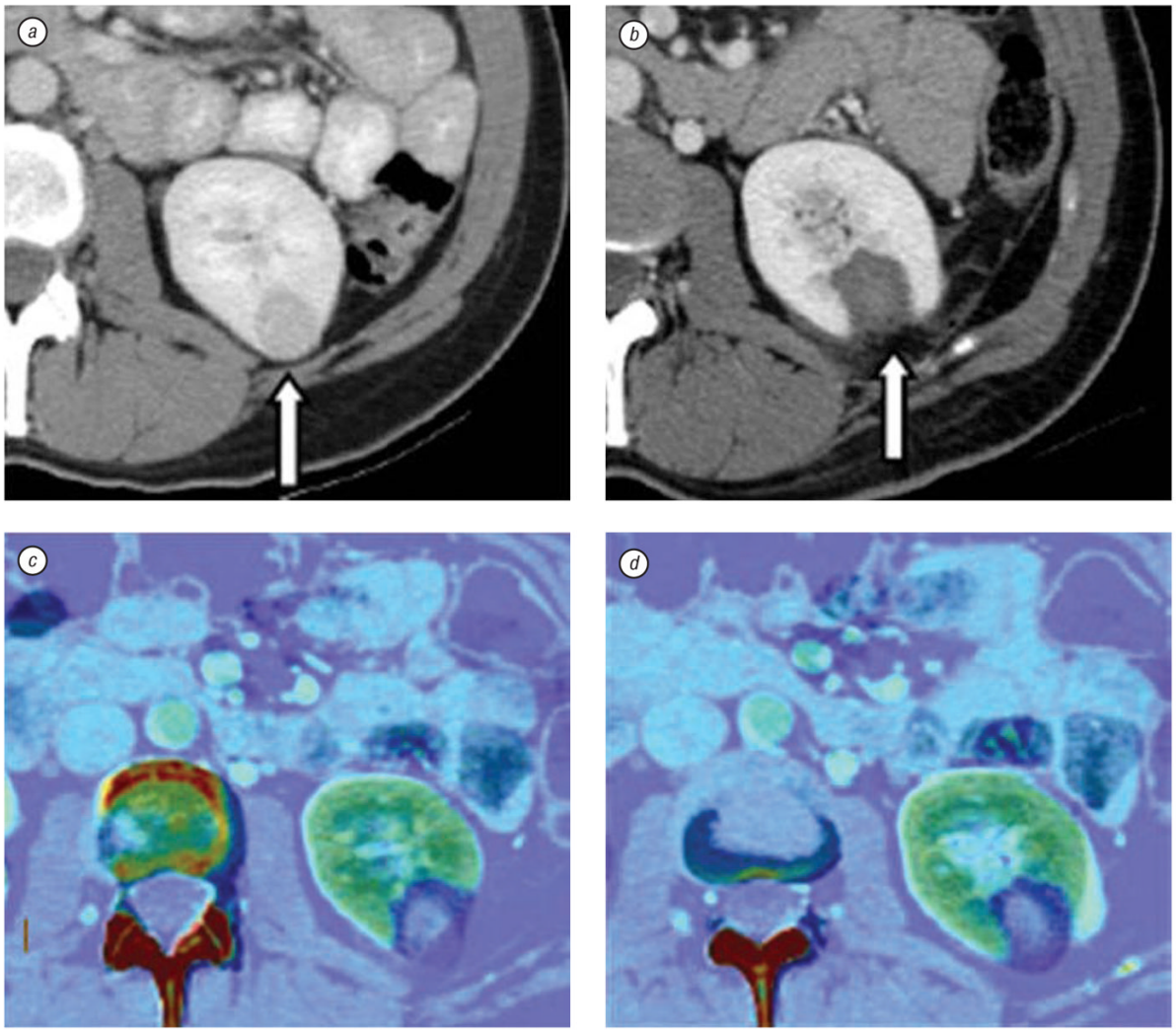

Fig. 3.

CT scan and elastic fusion images of kidney tumor and post-RFA thermal lesion. Contrast enhanced axial CT slices show a left kidney lesion before RFA (*a*, arrow) and thermal lesion two months after RFA (*b*, arrow). Due to change in kidney shape post ablation, elastic registration method is used to fuse pre- and post-RFA images (*c* and *d*), which defines treatment margins (dark blue)

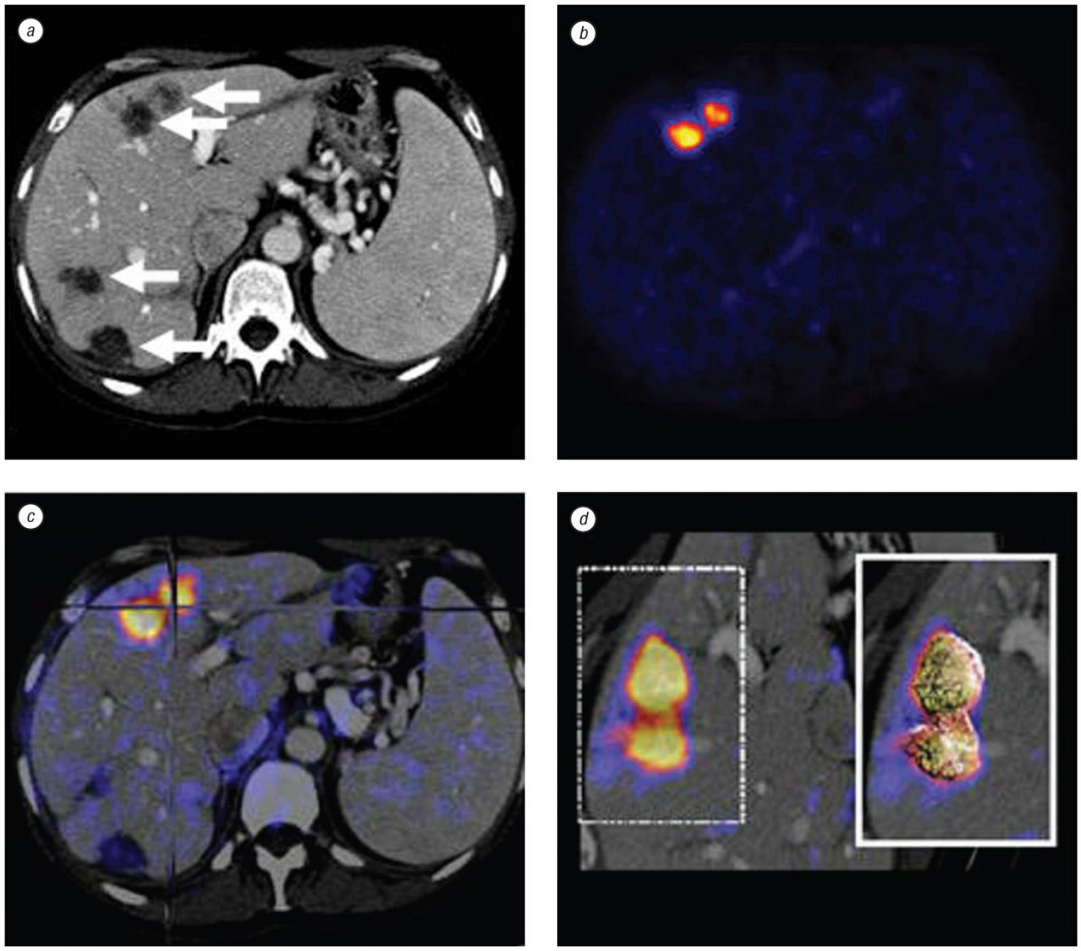

Fig. 4.

Patient with metastatic pancreatic carcinoma isolated to the liver. Pre-RFA contrast enhanced axial CT slice (*a*) shows detailed morphology with 4 possible targets (arrows) for treatment. PET (*b*) shows abnormal FDG uptake in 2 anterior liver lesions. Intermodality PET/CT fusion (*c*) localizes active lesions (crosshairs). Volume rendering (*d*) visualizes metabolic activity with 3 dimensional details

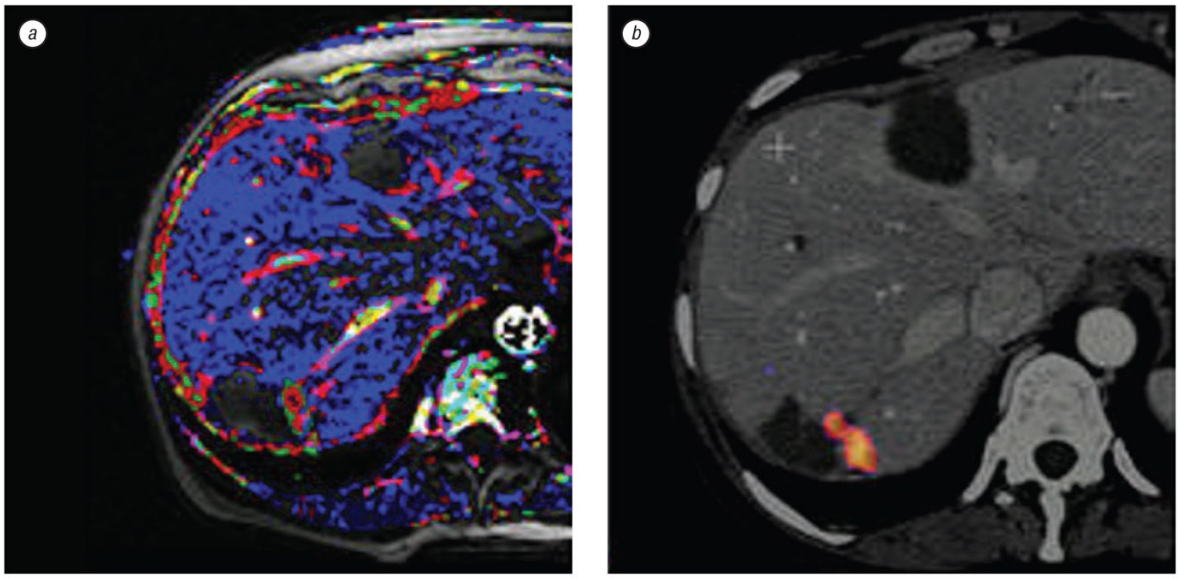

Fig. 5.
Patient with residual tumor following RFA for multiple liver metastases. Dynamic contrast enhanced MRI (*a*) compared to a fused PET/CT (*b*) confirms tumor and correlates vascular pharmacokinetics with metabolic activity

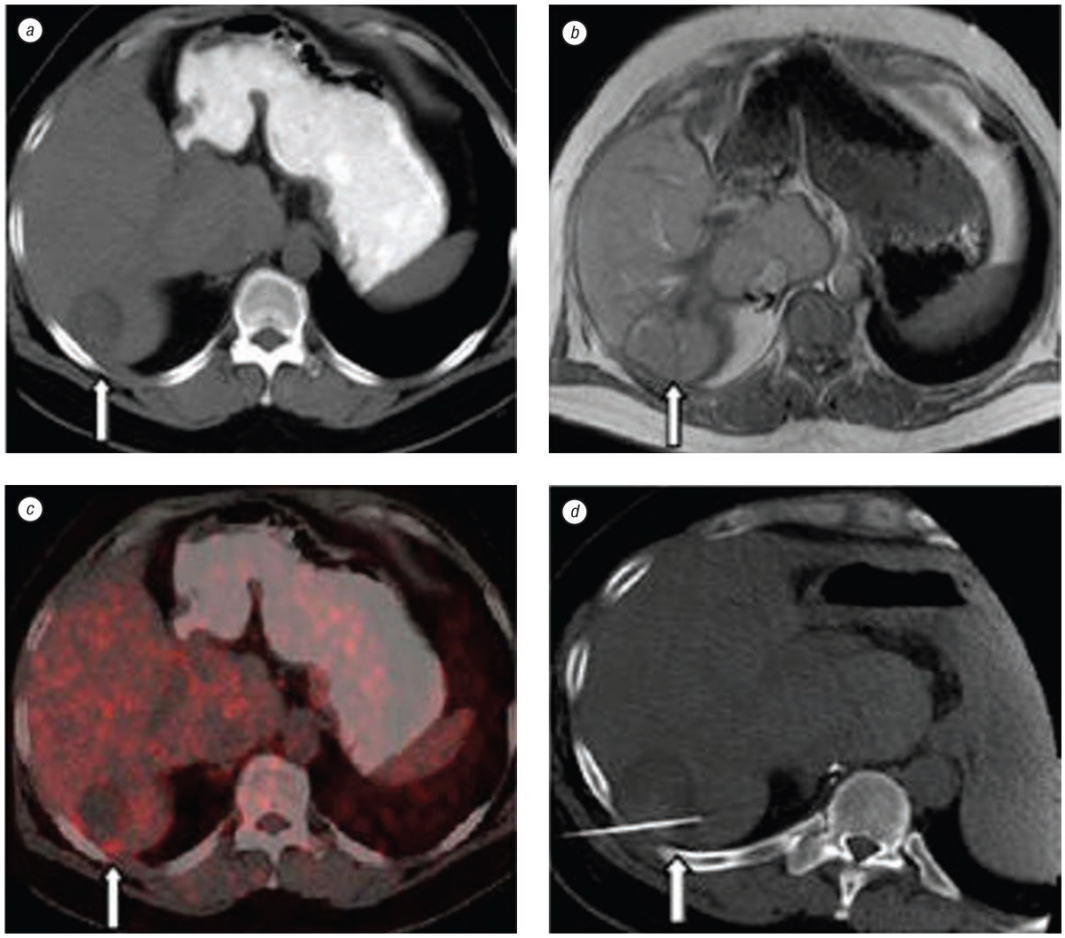

Fig. 6.
CT, MRI, and PET images of a patient with colorectal carcinoma with liver metastases. Axial CT (*a*) and MRI (*b*) slices post-RFA showing only morphology (arrows) appearing negative for recurrence. Retrospective off-line fusion of CT and PET data sets (*c*) validates a pathology-proven residual tumor along the posterior border of the liver. Repeat treatment targeted with spatial knowledge of PET activity (*d*)

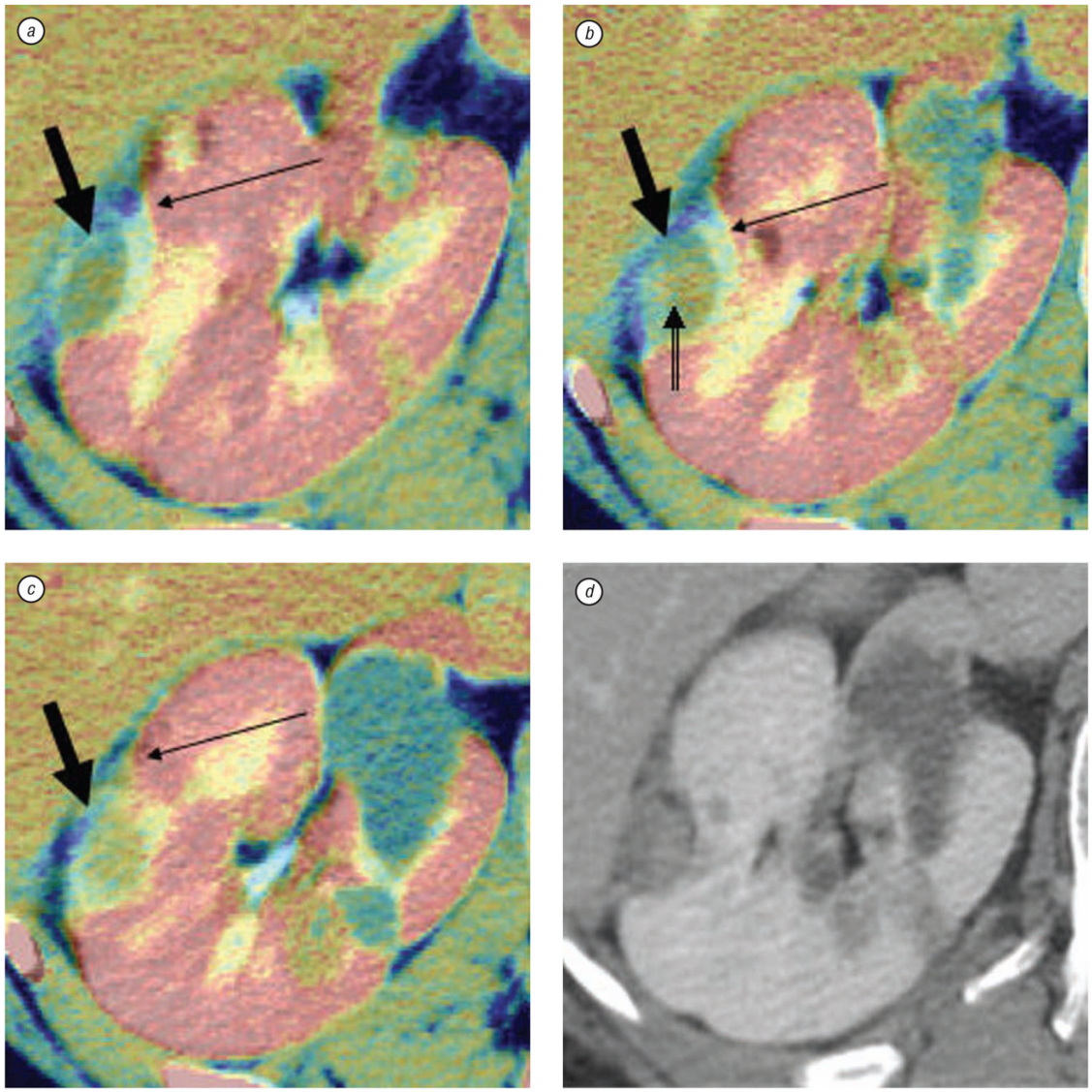

Fig. 7.

Right kidney tumor in patient with von Hipple-Lindau syndrome. Pre-RFA fused with post-RFA contrast enhanced axial CT slices (from superior to inferior, *a–c*) using optimized automated registration (OAR) method with correlation ratio voxel-similarity cost function. Images *a–c* were cropped and colorized with MIPAV tools to speed the registration process and enhance visualization. The pre-treatment CT appears in gray and the post-treatment CT is in color, i. e. the yellow treatment margin (thin arrows) overlays the original grayscale tumor (thick arrows). Notice the thin margin (double tailed arrow) in (*b*) which could potentially have been a site of recurrence; however, 6 month, 1 year, and 18 months (*d*) post treatment scans showed no recurrence. Although there was a thin margin, fusion correctly depicted an adequate thermal lesion

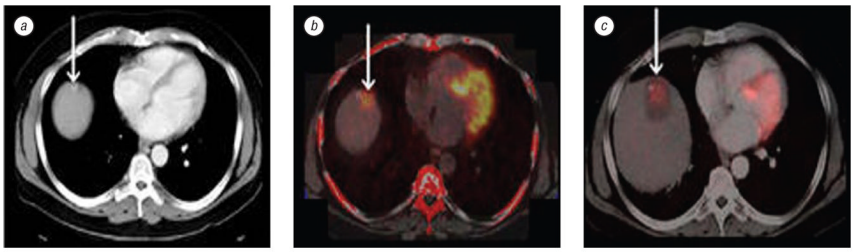

Fig. 8.

Patient with lesion at liver dome. Contrast enhanced axial CT slice shows low attenuation lesion adjacent to a high attenuation lesion (arrow) in dome of liver (*a*). Rigid registration of PET/CT pre-RFA shows abnormal FDG uptake over low attenuation lesion adjacent to high attenuation lesion (*b*). Post-RFA CT fused with pre-RFA PET (*c*) verifies RFA treatment zone with margins covering the area of abnormal FDG uptake (arrow)

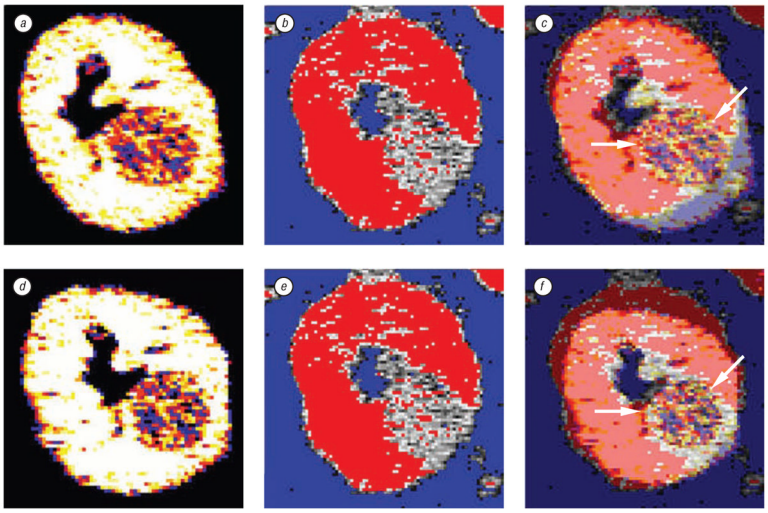

Fig. 9.

Post processed cropped and colorized CT before RFA, after RFA, and fused image using rigid and elastic registration methods. Top row (*a–c*) is rigid registration whereas the bottom row (*d–f*) is elastic registration. The first column (*a*, *d*) is pre-RFA CT. The second column (*b*, *e)* is 2 months post RFA CT scan. Rigid registration (*c*) matches hand picked anatomy from one image to the other without altering either source image. This may result in mismatch (arrow) since the organ has shifted in the time interval between imaging. Elastic registration (*f*) also uses landmarks for point-to-point registration, but allows deformation of anatomy to better match the area of interest (arrow)